

Are your MRI contrast agents cost-effective?

Learn more about generic Gadolinium-Based Contrast Agents.



FRESENIUS  
KABI

caring for life

# AJNR

## Current and Emerging MR Imaging Techniques for the Diagnosis and Management of CSF Flow Disorders: A Review of Phase-Contrast and Time–Spatial Labeling Inversion Pulse

This information is current as of April 17, 2024.

S. Yamada, K. Tsuchiya, W.G. Bradley, M. Law, M.L. Winkler, M.T. Borzage, M. Miyazaki, E.J. Kelly and J.G. McComb

*AJNR Am J Neuroradiol* 2015, 36 (4) 623-630

doi: <https://doi.org/10.3174/ajnr.A4030>

<http://www.ajnr.org/content/36/4/623>

# Current and Emerging MR Imaging Techniques for the Diagnosis and Management of CSF Flow Disorders: A Review of Phase-Contrast and Time–Spatial Labeling Inversion Pulse

S. Yamada, K. Tsuchiya, W.G. Bradley, M. Law, M.L. Winkler, M.T. Borzage, M. Miyazaki, E.J. Kelly, and J.G. McComb



## ABSTRACT

**SUMMARY:** This article provides an overview of phase-contrast and time–spatial labeling inversion pulse MR imaging techniques to assess CSF movement in the CNS under normal and pathophysiological situations. Phase-contrast can quantitatively measure stroke volume in selected regions, notably the aqueduct of Sylvius, synchronized to the heartbeat. Judicious fine-tuning of the technique is needed to achieve maximal temporal resolution, and it has limited visualization of CSF motion in many CNS regions. Phase-contrast is frequently used to evaluate those patients with suspected normal pressure hydrocephalus and a Chiari I malformation. Correlation with successful treatment outcome has been problematic. Time–spatial labeling inversion pulse, with a high signal-to-noise ratio, assesses linear and turbulent motion of CSF anywhere in the CNS. Time–spatial labeling inversion pulse can qualitatively visualize whether CSF flows between 2 compartments and determine whether there is flow through the aqueduct of Sylvius or a new surgically created stoma. Cine images reveal CSF linear and turbulent flow patterns.

**ABBREVIATIONS:** CSP = cavum septi pellucidi; NPH = normal pressure hydrocephalus; PC = phase-contrast; Time-SLIP = time–spatial labeling inversion pulse;  $V_{enc}$  = velocity-encoding value

Rapid advances in imaging techniques have remarkably improved the diagnosis and treatment of CNS disorders, with MR imaging being the most recent. New MR imaging applications are continually being developed, providing improved assessment of CNS disorders and their response to treatment. One area that has received much attention, but with only limited success, is CSF movement, the alteration of which results in many clinical disorders with hydrocephalus (including normal pressure hydrocephalus), cystic CSF collections, and Chiari malformations being more common. Until now, the only MR imaging technique to

visualize CSF movement is phase-contrast (PC) MR imaging. Time–spatial labeling inversion pulse (Time-SLIP) is another option, which makes it possible to noninvasively select CSF at any region in the CNS and visualize its movement for up to 5 seconds, providing information about CSF dynamics even in slow-flowing regions. Time-SLIP is expected to have widespread application for diagnosis and evaluation of response to treatment of abnormal CSF movement. The objective of this article is to review the history and findings of PC and discuss additional benefits of Time-SLIP as another technique for expanding the role of MR imaging for the care and management of CNS disorders.

From the Department of Neurosurgery (S.Y.), Toshiba Rinkan Hospital, Sagami-hara, Kanagawa, Japan; Department of Radiology (K.T.), Kyorin University, Mitaka, Tokyo, Japan; Department of Radiology (W.G.B.), University of California, San Diego, San Diego, California; Department of Neuroradiology (M.L.), University of Southern California, Los Angeles, California; Steinberg Diagnostic Imaging Center (M.L.W.), Las Vegas, Nevada; Division of Neuroradiology (M.T.B.), Department of Radiology, Institute for Maternal Fetal Health, Children's Hospital Los Angeles, Los Angeles, California; Department of Biomedical Engineering (M.T.B.), USC Viterbi School of Engineering, University of Southern California, Los Angeles, California; Toshiba Medical Research Institute (M.M.), Vernon Hills, Illinois; Toshiba America Medical Systems Inc (E.J.K.), Tustin, California; Division of Neurosurgery (J.G.M.), Children's Hospital Los Angeles, Los Angeles, California; and Department of Neurological Surgery (J.G.M.), Keck School of Medicine, University of Southern California, Los Angeles, California.

Please address correspondence to Erin J. Kelly, PhD, Toshiba America Medical Systems Inc, 2441 Michelle Dr, Tustin, CA 92780; e-mail: ekelly@tams.com

Indicates open access to non-subscribers at [www.ajnr.org](http://www.ajnr.org)

Indicates article with supplemental on-line appendix.

Indicates article with supplemental on-line video.

<http://dx.doi.org/10.3174/ajnr.A4030>

## Phase-Contrast MR Imaging: Technical Review

The earliest MR imaging visualization of CSF flow through the aqueduct was not obtained through quantitative methods but was inferred through distinct MR imaging flow artifacts arising from decreased signal and magnified by increased flow velocities.<sup>1–4</sup> Initial methods for quantifying such flow relied on knowledge of the T1 and T2 relaxation times of the CSF or a comparison of the degree of saturation between static tissue and flowing regions.<sup>5,6</sup> Later a modified gradient-echo technique, using phase shifts induced by bipolar gradients programmed into the pulse sequence, improved visualization of CSF movement. Feinberg and Mark<sup>7</sup> implemented a velocity imaging method that combined cardiac synchronization, 2D Fourier transform phase-encoding, and high temporal resolution to measure brain motion and CSF flow. They found differences in CSF velocity patterns in patients with dilated

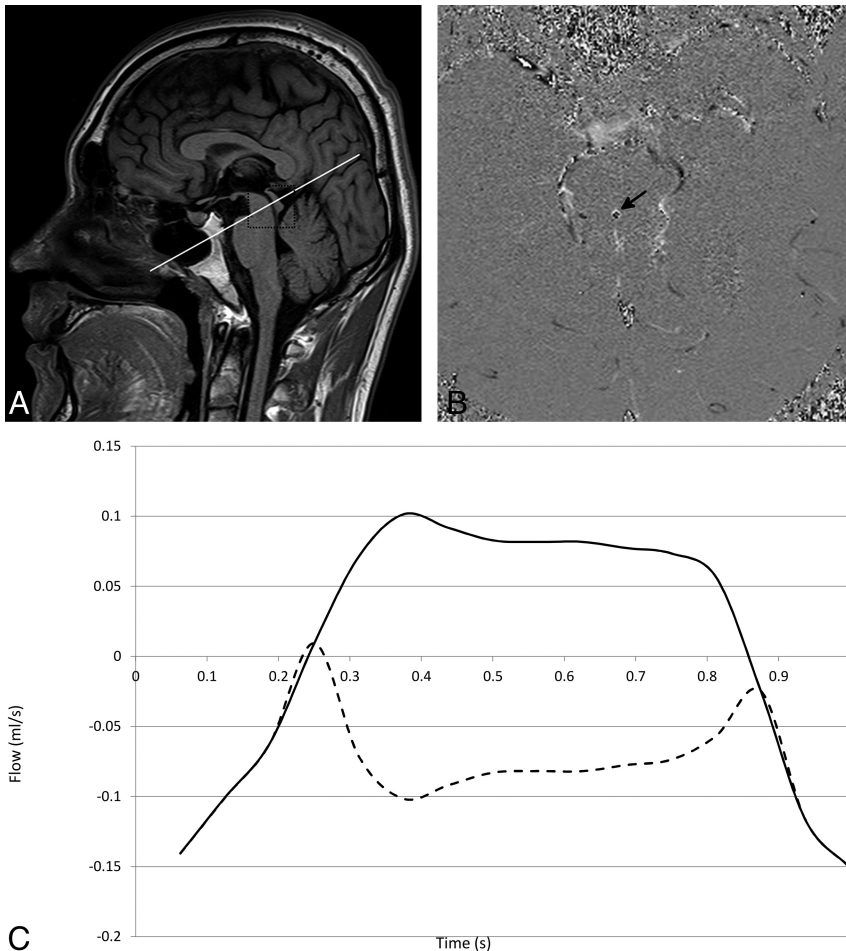


**FIG 1.** A 26-year-old healthy male volunteer. A, Geometry for the oblique-axial CSF phase-contrast scan. The section is positioned axially at a  $90^\circ$  angle through the aqueduct of Sylvius (rectangle, A). Aliasing (B) occurs if a phase value is greater than the maximum expected velocity, causing the phase to wrap back to a multiple of  $\pi$ , appearing black (black arrow) when it should appear white (or vice versa). Uncorrected (dotted line) and corrected (solid line) flow waveforms in milliliters per second represent bidirectional flow through the aqueduct (C). Aliasing can be corrected off-line by adding a multiple of  $2 \times \pi \times V_{\text{enc}}$  to aliased pixels.

ventricles compared with controls, an early indication that MR velocity imaging might be useful in evaluating hydrocephalus.<sup>7</sup>

In PC, signal contrast between flowing and stationary spins is generated by sensitizing the phase of the transverse magnetization to the velocity of the spins.<sup>8,9</sup> PC collects 2 datasets, each with opposite polarity. When the 2 datasets are subtracted, accumulated phases from stationary spins cancel, but because flowing spins move from 1 position in the magnetic field gradient to another during the time between the executions of the 2 opposite polarity gradients, the moving spins accumulate a net phase proportional to the velocity of the nuclei. Because velocity is being measured as phase, the velocity values must be within  $+\pi$  and  $-\pi$ . Aliasing occurs if a phase value is  $>\pi$ , causing the phase to wrap back to a multiple of  $\pi$ .

A parameter was developed that sets the maximum velocity that can be encoded in the pulse sequence, known as the velocity-encoding value ( $V_{\text{enc}}$ ). The  $V_{\text{enc}}$  can be adjusted according to the arrangement of the bipolar gradients. PC generates the best results when maximum flow velocity is anticipated correctly through the

$V_{\text{enc}}$ . Flow velocities greater than the  $V_{\text{enc}}$  produce aliasing artifacts, and velocities much smaller than the  $V_{\text{enc}}$  result in poor image quality and weak signal.<sup>10,11</sup> An example of aliasing artifacts is shown in Fig 1. When aliasing occurs, the velocity information must be corrected by adding or subtracting  $2 \times \pi \times V_{\text{enc}}$  during postprocessing, or the scan can be repeated with a higher  $V_{\text{enc}}$ . Magnitude and phase images are generated from 1 acquisition containing both anatomy and velocity information.

By synchronizing the acquisition with the cardiac cycle, the series of images generated contains velocity information that can be mapped to the phases of the heartbeat. From this, velocity can be plotted as a function of the cardiac cycle, providing the ability to calculate stroke volume, flow rate, mean velocity, and peak systolic/diastolic flow. Two series of velocity images are shown in Fig 2, where Fig 2A depicts a series of midline sagittal images and Fig 2B depicts a series of axial images at the level of the aqueduct. In both series, every odd phase of the 16 cardiac phases that were acquired is displayed.

### PC and CSF Imaging

The SNR in PC images is highly related to the precision between the  $V_{\text{enc}}$  and the velocity being measured. Choosing the  $V_{\text{enc}}$  very close to the maximum expected velocity results in the maximum SNR in the velocity image. The  $V_{\text{enc}}$  must be lowered to achieve sufficient SNR for slow CSF flow. A setting of a  $V_{\text{enc}}$  that is too low may cause aliasing. Lowering the  $V_{\text{enc}}$  increases the gradient strength on the bipolar

gradient and may increase the TR. Imaging flow throughout the cardiac cycle requires a short TR to achieve adequate temporal resolution. Therefore, PC for optimal CSF flow results requires careful fine-tuning of parameters for maximizing temporal resolution, SNR, and  $V_{\text{enc}}$ . This sometimes can be problematic for patients whose CSF flow velocities are very high or very low compared with control values, with no way to individually predetermine the optimal situation. PC can only measure CSF if it is moving.

One limitation of the measurements obtained from PC acquisitions is that they result from data collected over a large number of cardiac cycles. The final velocity waveform represents an average measurement of those cycles, but it is presented as 1 cycle. For the most accurate quantitative evaluation of CSF flow, through-plane acquisition is performed perpendicular to the aqueduct, which minimizes partial volume effects.<sup>10,11</sup> Qualitative assessment of CSF flow can be accomplished with a midline sagittal acquisition for assessing in-plane flow. Not accounted for is the effect of respiration.

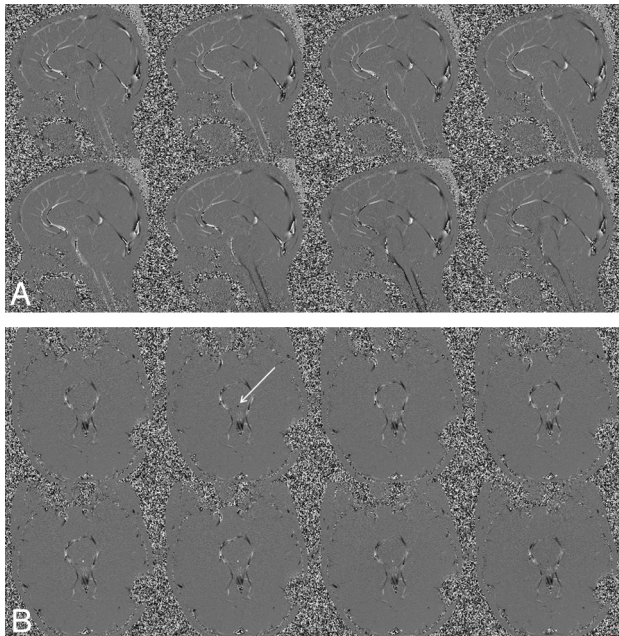


**FIG 2.** An 18-year-old healthy female volunteer. *A*, A series of midline sagittal images depicting pulsatile CSF flow, where flow magnitude and direction are represented as gray-scale. Flow changes from positive to negative and back to positive (white indicates peak caudal flow; black, peak cranial flow). *B*, Depiction of a series of axial images at the level of the aqueduct (arrow). In both series, every odd phase of the 16 cardiac phases that were acquired is displayed.

### Quantitative Measurements from PC

Since the development of PC, clinical MR imaging flow studies of CSF have primarily focused on measurements in the aqueduct; however, a few studies sought to quantify flow in the prepontine cistern and craniocervical junction.<sup>12-14</sup> CSF pulsatility has been studied extensively by using this method<sup>15,16</sup> and has successfully demonstrated the ability to quantify CSF in axial locations throughout the brain. The pulsatile component moves cranially and caudally in a cyclical fashion as a function of the cardiac cycle at aqueductal peak velocity between 3 and 7 cm/s.<sup>14</sup> On the basis of these CSF flow studies, the brain is considered to behave as if it were being pulled in systole by the spinal cord secondary to arterial expansion.<sup>15</sup>

Numerous studies have documented normal aqueductal stroke volumes between 30 and 50  $\mu\text{L}$ .<sup>14,15,17,18</sup> (The aqueductal CSF stroke volume is defined as the average of the volume flowing down during systole and up during diastole.<sup>19</sup>) Studies of CSF flow in hydrocephalus secondary to intracranial pressure changes demonstrated by invasive monitoring have found up to a 10-fold increased pulsatile aqueductal flow<sup>15,17,19-24</sup> compared with that in healthy controls. This finding has been used to build criteria for diagnosing idiopathic normal pressure hydrocephalus (NPH) based on stroke volumes of  $>42 \mu\text{L}$ <sup>19</sup> or pulsatile flow rates above a threshold of 18 mL/min, for example.<sup>20</sup> However, setting thresholds such as these has so far not proved to be clinically reliable. For example, Greitz<sup>15</sup> found, along with an increased aqueductal flow rate, a corresponding decreased flow rate through the craniocervical junction. Balédent et al,<sup>12</sup> in a larger study, found no such changes. To use stroke volume to diagnose hyperdynamic CSF, a measurement that some investigators have

advocated for diagnosing shunt-responsive NPH,<sup>19</sup> one must first determine a baseline stroke volume in healthy elderly patients. Then, by using the same technique on the same machine, some have found a stroke volume twice normal to correlate with shunt responsiveness.<sup>19</sup>

In addition to net flow measurements, some studies have used the time-dependent features of the waveform to identify abnormal pathophysiology. One such study revealed a shorter systolic flow period of the temporal waveform for patients with communicating hydrocephalus compared with healthy controls.<sup>12</sup> PC measurements of CSF flow have also been used to study patients with Chiari I malformation. In these studies, the CSF flow at the craniocervical junction has been shown to exhibit changes in flow patterns, including local flow jets and bidirectional flow.<sup>25-27</sup> These studies have shown that patients with Chiari I malformations have significant elevations of peak CSF systolic velocity at the foramen magnum. The application of these findings to determine which patients would benefit from a craniocervical decompression has, however, proved problematic.

PC has also been used to study vascular flow timing with respect to CSF flow timing in various locations in the brain. Some studies hypothesized that vascular flow timing may be used as a measure of intracranial compliance changes in NPH and can be used as an indicator of shunt responsiveness.<sup>28</sup> These studies have not proved helpful because the measurements were not able to successfully predict shunt responsiveness.<sup>29</sup> A study of PC measurements of hydrodynamics found that the patients who responded to shunts were identical to the nonresponders in all variables measured.<sup>29</sup>

Prediction of improved clinical function following CSF diversion, particularly in patients thought to have NPH, has been a highly sought goal for PC CSF flow studies. In particular, the association between aqueductal stroke volume and the response to shunting has been tested numerous times.<sup>19,21-24,30,31</sup> Initial studies found a positive response to CSF diversion for patients with NPH whose aqueductal stroke volumes reached  $\geq 42 \mu\text{L}$ .<sup>19</sup> However, repeat studies by Kahlon et al<sup>32</sup> performed in 38 patients did not find any statistical significance between stroke volume and improvement from shunting. Dixon et al<sup>22</sup> also failed to find an association between CSF pulsatility and clinical symptoms of NPH. Some of the variability in findings may be attributed to temporal changes that naturally occur, with PC measuring 1 point in time of a dynamically changing system. In fact, Scollato et al<sup>33</sup> observed a patient with unshunted hydrocephalus for 2 years and found an initial increase in aqueductal stroke volume, followed by a decrease. Therefore, this variability in pulsatility, which is still not clearly understood, makes it difficult to use a single PC measurement of stroke volume as a reliable predictor of whether a given patient will respond favorably to CSF diversion.

### Time-SLIP

**A New Look at CSF Movement.** Historic CSF flow theories of progressive hydrocephalus propose that blockage of the arachnoid granulations increases the resistance to the absorption of CSF into the bloodstream, leading to an accumulation of CSF in the ventricles. In the pulsatile models of hydrocephalus, a “water-hammer” effect is hypothesized, in which large undamped pul-



sations produce increased pressure gradients and asymmetric pulsation distributions lead to ventricular dilation.<sup>34,35</sup> Enlarged pulse-wave amplitudes of CSF movement in patients with NPH have been observed and measured with MR imaging for a number of years.<sup>1,36</sup> This effort has attempted to improve our understanding of hydrocephalus.<sup>14,15,36</sup> However, it has failed to correctly identify those patients who would benefit from CSF diversion. PC cannot reliably visualize CSF flow within the ventricular or subarachnoid spaces or within cysts; this visualization can be repeatedly accomplished with Time-SLIP.<sup>37</sup> Bulk CSF flow (ie, drainage of CSF from the CNS) of approximately 20 mL/h, is too little and too widely dispersed to be seen with MR imaging at present.

**Time-SLIP and Arterial Spin-Labeling.** Time-SLIP is an arterial spin-labeling variant that can be combined with fast advanced spin-echo or steady-state free precession sequences to depict flow in any imaging orientation within a targeted region.<sup>37,38</sup> For vascular imaging, arterial spin-labeling magnetically tags the blood with radio frequency pulses and uses the labeled blood as a tracer to generate vascular images in a relatively simple manner. The stationary tissue signal is suppressed by an inversion pulse, and the final image contains only the contribution of the labeled flow, acquired after a deliberate delay time known by convention as the TI interval. Arterial spin-labeling has been used to evaluate blood flow in the renal, carotid, and pulmonary arteries and in the pulmonary and portal-venous systems. This technique produces high-quality angiograms by using blood as its own tracer, instead of a contrast agent.<sup>39-44</sup> The application of arterial spin-labeling lends itself very well to imaging CSF movement, by using CSF as its own tracer as well.

**Time-SLIP and CSF.** CSF is a flowing entity; therefore, a similar approach can be used to depict CSF movement, but in a unique way. Unlike PC, which is cardiac-gated and displays the visualization of the pulsatile component of CSF, 2D Time-SLIP acquisitions are incremental, allowing the linear and turbulent movement components of CSF to be seen for up to 5 seconds noninvasively for the first time. Using a 2D fast advanced spin-echo sequence as the fundamental acquisition scheme, Time-SLIP can acquire a series of single-shot images with incremental TI to visualize linear and turbulent flow.<sup>37</sup>

**Time-SLIP: Technical Review.** CSF movement viewed with Time-SLIP uses a single-shot fast advanced spin-echo technique as the underlying sequence in any sagittal, coronal, axial, or oblique plane. Technical details can be found in the article by Yamada et al.<sup>37</sup> While the use of arterial spin-labeling for visualization of the vasculature throughout the body is well-established, its application for CSF flow imaging is relatively new and differs from traditional applications in its use of incremental TI within the same 2D imaging sequence, thus enabling the CSF and its movement to be viewed in small incremental steps, independent of the cardiac cycle.

### **Distinguishing CSF Flow Patterns**

Time-SLIP has enabled CSF flow to be viewed and understood in a new way that has directly benefitted patients.<sup>45,46</sup> On the basis of a number of studies using Time-SLIP on healthy subjects, it has showed evidence of turbulent reflux flow between the aqueduct of

Sylvius and the third ventricle, something that has never been seen on PC.<sup>37</sup> In addition, this reflux flow was also clearly and consistently seen in the lateral ventricles because CSF flows backward from the third ventricle through the foramen of Monro into the lateral ventricle.<sup>37</sup>

On the basis of the results of initial baseline studies, Time-SLIP can be readily used as a screening tool to determine whether the CSF flow is typical, atypical, or not moving at all.<sup>37</sup> In an article by Yamada et al,<sup>37</sup> 2 patients with hydrocephalus did not exhibit the same reflux pattern consistently depicted in the healthy subjects. In a patient with noncommunicating hydrocephalus secondary to a posterior fossa tumor, the reflux flow into the lateral ventricle was absent from the tagged CSF in the third ventricle. A repeat study in this patient following the placement of a right lateral ventricle external CSF drain showed re-establishment of the normal reflux flow pattern consistently observed in the healthy subjects. In a patient with a left middle fossa arachnoid cyst, the CSF in the basal cistern was tagged. Before fenestration, no evidence of CSF flow into the cyst was noted. After surgical intervention, a repeat study demonstrated labeled CSF flowing into the cyst. In both cases, imaging with Time-SLIP confirmed noninvasively the anticipated restoration of CSF movement.

A recent case study reported the usefulness of Time-SLIP in evaluating a patient with an enlarging symptomatic cavum septi pellucidi (CSP), a CSF-filled cavity bounded by thin triangular vertical membranes separating the right and left anterior horns of the lateral ventricles.<sup>47</sup> Serial CT scans noted progressive enlargement of the CSP and lateral ventricles in this patient, who developed progressive headaches and obtundation following a subarachnoid hemorrhage. Before surgical intervention, Time-SLIP showed CSF flow between the third and lateral ventricles, but not into the CSP. Following surgical fenestration of the CSP, MR imaging with Time-SLIP demonstrated decreased ventricular and CSP size and the presence of CSF flowing between the third ventricle and the CSP, which coincided with resolution of this patient's symptoms. The Time-SLIP study in this patient supported the hypothesis of Shaw and Alvord<sup>48</sup> that in asymptomatic non-expanding CSP, CSF is in free communication with the ventricular system. In fact, the study showed that when CSF communication was absent in this patient, the CSP expanded.<sup>48</sup> The case study is an example of the clinical usefulness of the technique in demonstrating the presence or absence of CSF communication.

The effect of respiration on CSF flow has not been adequately studied with PC because of temporal limitations. Low-resolution or indirect methods such as echo-planar imaging and real-time acquisition and evaluation of pulsatile blood flow have not been able to adequately visualize CSF movement in response to respirations either.<sup>49</sup> The higher intrinsic SNR and temporal resolution of Time-SLIP make it possible to visualize CSF movement in response to respiration and how the CSF flow patterns are altered by the depth of the respiratory effort.

### **Utility of Time-SLIP**

Time-SLIP is a straightforward noninvasive method for determining whether CSF can flow between 2 spaces and whether flow has been restored after surgical intervention.<sup>37,47</sup> Because Time-

SLIP acquires a series of images during several seconds, the presence or absence of CSF movement from the tagged region into adjacent compartments, such as through the aqueduct of Sylvius,

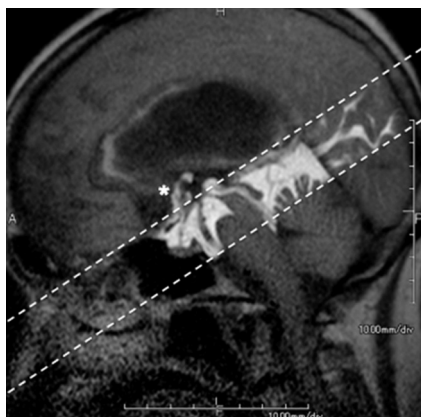


**FIG 3.** Hydrocephalus in a 74-year-old woman. The patient had undergone endoscopic third ventriculostomy. Patency of the fenestration on the floor of the third ventricle is readily and noninvasively confirmed postsurgery by the presence of CSF flow between the third ventricle and the basal cisterns (*asterisk*) emerging from the tagged region (*dotted lines*). (See On-line Video 1, which demonstrates postsurgical CSF flow between the third ventricle and the basal cisterns.)

confirms the presence of CSF flow or blockage, as seen in the patient depicted in Fig 3, before and after endoscopic third ventriculostomy. Time-SLIP can be used postoperatively to evaluate the patency of the fenestration by observing CSF flow between the third ventricle and the basal cisterns (Fig 3). Reflux flow from the third ventricle into the lateral ventricle has been established in adult patients without hydrocephalus; however, flow has been shown to be restricted in patients with hydrocephalus and NPH.<sup>37</sup> Normal reflux flow in a healthy patient is seen in Fig 4A, restricted in NPH (Fig 4B), and restored after surgical intervention (Fig 4C). A Chiari malformation can restrict normal CSF flow between the cranial and spinal compartments; this restriction, in turn, results in CSF accumulation within the spinal cord, producing a syrinx. Time-SLIP is a useful, noninvasive tool for evaluating pre- and postoperative craniocervical decompressive changes to CSF flow (Fig 5).

For understanding CSF flow disorders, the PC technique to quantify CSF flow velocities and Time-SLIP to visualize CSF flow characteristics, pathways, and blockages are qualitatively useful techniques in combination. Time-SLIP is especially useful in regions where it is difficult or impossible to visualize CSF flow with PC, such as in the lateral ventricles, subarachnoid spaces, or within a cyst, secondary to limitations of  $V_{enc}$ , SNR, or the absence of pulsatile flow. The Time-SLIP tag is freely selectable, and

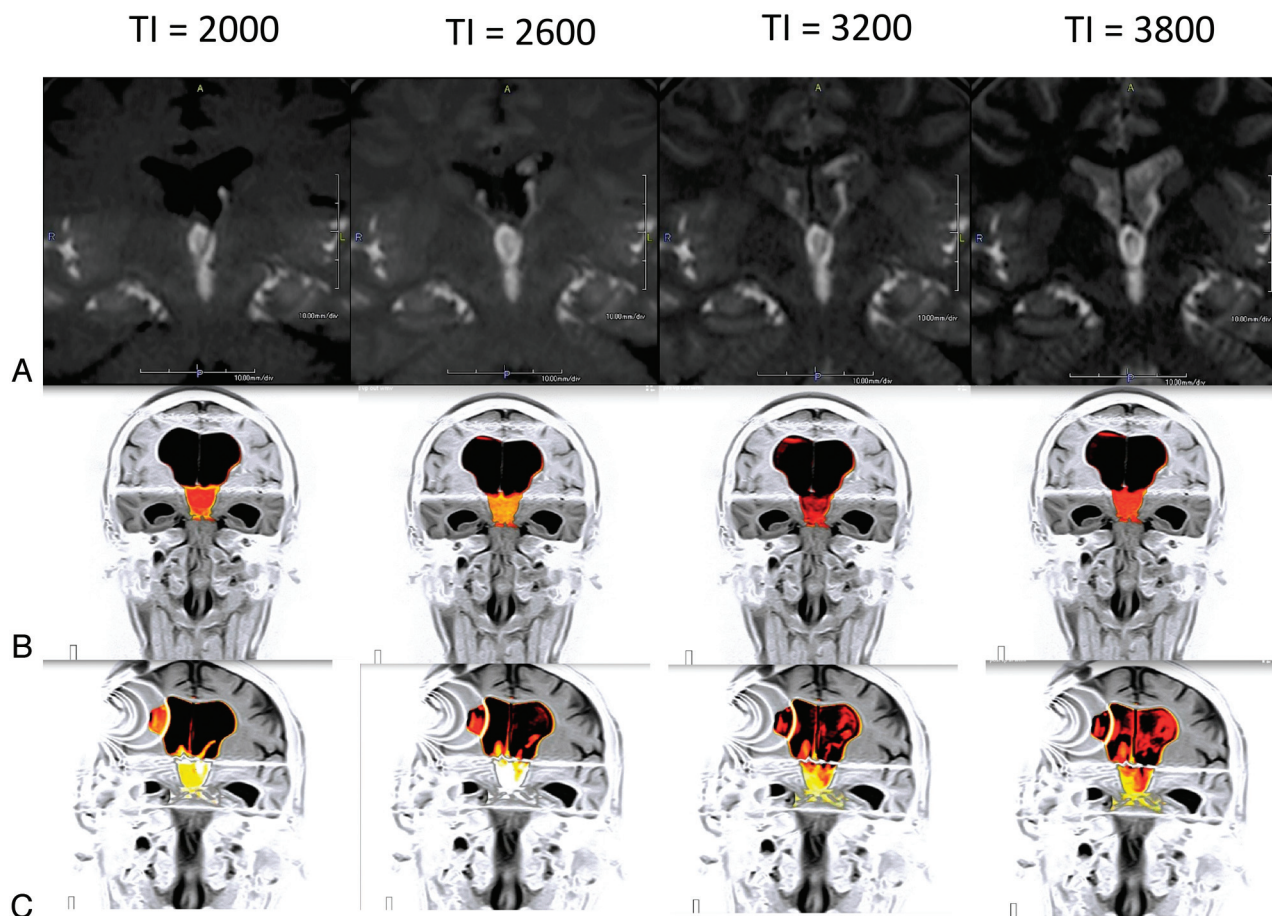


**FIG 4.** Idiopathic normal pressure hydrocephalus in a 78-year-old man. Time-SLIP has consistently shown the presence of reflux flow from the third ventricle into the lateral ventricle in adult patients without hydrocephalus (A). This flow is shown to be restricted in NPH (B). Time-SLIP in the same patient confirms that this flow is restored after surgical intervention by inserting a CSF diverting shunt (C, artifacts on the right are from the shunt valve). (See On-line Videos 2 and 3, which demonstrate restricted flow and restored flow pre- and postsurgery, respectively.)



TI 1800

TI 2500

TI 3200

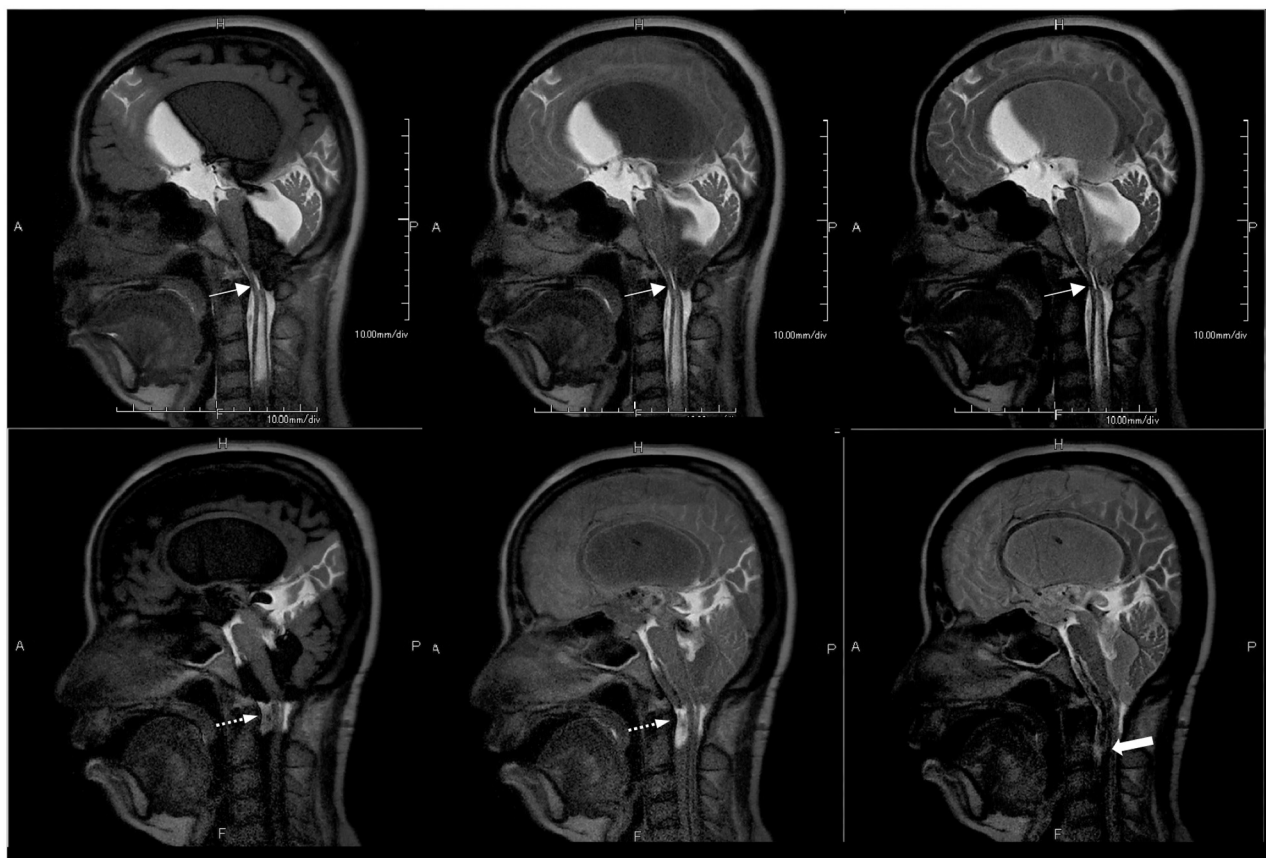


**FIG 5.** Chiari malformation in a 43-year-old woman pre- (top row) and post- (bottom row) surgery, shown at incremental TIs. Obliteration of the subarachnoid space at the craniocervical junction is associated with Chiari I malformation and a syrinx (top row, *arrow*). Following craniocervical decompression (bottom row, *arrow*), Time-SLIP shows CSF flow ventral to the brain stem and cervical spinal cord and a decrease in the size of the syrinx (*bold arrow*). (See On-line Videos 4 and 5, which demonstrate restricted flow and restored flow with a decrease in the size of the syrinx pre- and postsurgery, respectively.)

its orientation is easily and infinitely changed to target the region of interest, allowing CSF flow to be visualized in any direction or location.

Half of all occurrences of NPH have no known cause, and diagnosis is made primarily by clinical observations such as gait disturbances, dementia, and incontinence. Although enlarged ventricles are the expected MR imaging finding in patients with suspected NPH, the definitive diagnosis of NPH is difficult, and PC has not consistently predicted patient responsiveness to shunting. More extensive studies are currently underway to investigate whether Time-SLIP will be more predictive in diagnosing suspected NPH that is responsive to CSF diversion.

Time-SLIP can be used to determine whether CSF spaces are in communication. Following an endoscopic third ventriculostomy, a catheter is often placed in the ventricle to measure postoperative intraventricular pressure. Contrast injected into the ventricles can establish the success of the procedure by noting the distribution of the contrast with a CT scan. The use of Time-SLIP for this purpose would alleviate the need for postprocedural CT ventriculography because surgical outcomes could be assessed noninvasively.<sup>37</sup>

### Summary and Future Work

PC was the first quantitative MR imaging tool for evaluating CSF in pathophysiologic conditions. Time-SLIP provides additional information about CSF flow patterns. Perhaps most remarkably, the typical CSF flow pathway that has been described in textbooks is actually much different from that observed noninvasively with Time-SLIP,<sup>45</sup> even in the normal, nonhydrocephalic brain. Larger clinical studies are expected to provide additional evidence. Possible clinical applications using Time-SLIP to visualize and monitor CSF movement are listed in the On-line Appendix.

Most treatments for hydrocephalus and related CSF flow disorders are surgical, and these are known to work well in appropriate patients. Initial Time-SLIP studies have shown that successful treatments can be attained by understanding CSF flow patterns and by restoring these flow patterns when they are abnormal.<sup>37,45,47</sup>

Disclosures: Shinya Yamada—UNRELATED: Grants/Grants Pending: \$5000,\* Payment for Lectures (including service on Speakers Bureaus): \$2000, Travel or Meeting Expenses Unrelated to Activities Listed: \$2000, all from Toshiba Medical Systems. Kazuhiro Tsuchiya—UNRELATED: Payment for Lectures (including service on Speakers Bureaus): Development of Educational Presentations: Toshiba Medical Systems. Mark L. Winkler—RELATED: Other: travel support to meetings from Toshiba Medical Systems; UNRELATED: Consultancy: Toshiba America Medical Systems. \*Money paid to the institution.

## REFERENCES

- Bradley WG Jr, Kortman KE, Burgoyne B. **Flowing cerebrospinal fluid in normal and hydrocephalic states: appearance on MR images.** *Radiology* 1986;159:611–16
- Mark AS, Feinberg DA, Sze GK, et al. **Gated magnetic resonance imaging of the intracranial cerebrospinal fluid spaces.** *Acta Radiol Suppl* 1986;369:296–99
- Bradley WG Jr, Whittemore AR, Kortman KE, et al. **Marked cerebrospinal fluid void: indicator of successful shunt in patients with suspected normal-pressure hydrocephalus.** *Radiology* 1991;178:459–66
- Krauss JK, Regel JP, Vach W, et al. **Flow void of cerebrospinal fluid in idiopathic normal pressure hydrocephalus of the elderly: can it predict outcome after shunting?** *Neurosurgery* 1997;40:67–73, discussion 73–74
- Singer JR. **Nuclear magnetic resonance blood flow measurements.** *Cardiovasc Intervent Radiol* 1986;8:251–59
- Singer JR, Crooks LE. **Nuclear magnetic resonance blood flow measurements in the human brain.** *Science* 1983;221:654–56
- Feinberg, DA, Mark, AS. **Human brain motion and cerebrospinal fluid circulation demonstrated with MR velocity imaging.** *Radiology* 1987;163:793–99
- Dumoulin CL, Yucel EK, Vock P, et al. **Two- and three-dimensional phase contrast MR angiography of the abdomen.** *J Comput Assist Tomogr* 1990;14:779–84
- Tsuruda JS, Shimakawa A, Pelc NJ, et al. **Dural sinus occlusion: evaluation with phase-sensitive gradient-echo MR imaging.** *AJNR Am J Neuroradiol* 1991;12:481–88
- Connor SE, O’Gorman R, Summers P, et al. **SPAMM, cine phase contrast imaging and fast spin-echo T2-weighted imaging in the study of intracranial cerebrospinal fluid (CSF) flow.** *Clin Radiol* 2001;56:763–72
- Saloner D. **The AAPM/RSNA physics tutorial for residents: an introduction to MR angiography.** *Radiographics* 1995;15:453–65
- Balédent O, Gondry-Jouet C, Meyer ME, et al. **Relationship between cerebrospinal fluid and blood dynamics in healthy volunteers and patients with communicating hydrocephalus.** *Invest Radiol* 2004;39:45–55
- Greitz D, Hannerz J, Rahn T, et al. **MR imaging of cerebrospinal fluid dynamics in health and disease: on the vascular pathogenesis of communicating hydrocephalus and benign intracranial hypertension.** *Acta Radiol* 1994;35:204–11
- Wagshul ME, Chen JJ, Egnor MR, et al. **Amplitude and phase of cerebrospinal fluid pulsations: experimental studies and review of the literature.** *J Neurosurg* 2006;104:810–19
- Greitz D. **Cerebrospinal fluid circulation and associated intracranial dynamics: a radiologic investigation using MR imaging and radionuclide cisternography.** *Acta Radiol Suppl* 1993;386:1–23
- Naidich TP, Altman NR, Gonzalez-Arias SM. **Phase contrast cine magnetic resonance imaging: normal cerebrospinal fluid oscillation and applications to hydrocephalus.** *Neurosurg Clin N Am* 1993;4:677–705
- Bateman GA, Levi CR, Schofield P, et al. **The pathophysiology of the aqueduct stroke volume in normal pressure hydrocephalus: can comorbidity with other forms of dementia be excluded?** *Neuroradiology* 2005;47:741–48
- Stoquart-ElSankari S, Balédent O, Gondry-Jouet C, et al. **Aging effects on cerebral blood and cerebrospinal fluid flows.** *J Cereb Blood Flow Metab* 2007;27:1563–72
- Bradley WG Jr, Scalzo D, Queralt J, et al. **Normal-pressure hydrocephalus: evaluation with cerebrospinal fluid flow measurements at MR imaging.** *Radiology* 1996;198:523–29
- Luetmer PH, Huston J, Friedman JA, et al. **Measurement of cerebrospinal fluid flow at the cerebral aqueduct by use of phase-contrast magnetic resonance imaging: technique validation and utility in diagnosing idiopathic normal pressure hydrocephalus.** *Neurosurgery* 2002;50:534–43, discussion 543–44
- Egeler-Peerdeman SM, Barkhof F, Walchenbach R, et al. **Cine phase-contrast MR imaging in normal pressure hydrocephalus patients: relation to surgical outcome.** *Acta Neurochir Suppl* 1998;71:340–42
- Dixon GR, Friedman JA, Luetmer PH, et al. **Use of cerebrospinal fluid flow rates measured by phase-contrast MR to predict outcome of ventriculoperitoneal shunting for idiopathic normal-pressure hydrocephalus.** *Mayo Clin Proc* 2002;77:509–14
- Poca MA, Sahuquillo J, Busto M, et al. **Agreement between CSF flow dynamics in MRI and ICP monitoring in the diagnosis of normal pressure hydrocephalus: sensitivity and specificity of CSF dynamics to predict outcome.** *Acta Neurochir Suppl* 2002;81:7–10
- Gideon P, Ståhlberg F, Thomsen C, et al. **Cerebrospinal fluid flow and production in patients with normal pressure hydrocephalus studied by MRI.** *Neuroradiology* 1994;36:210–15
- Houghton VM, Korosec FR, Medow JE, et al. **Peak systolic and diastolic CSF velocity in the foramen magnum in adult patients with Chiari I malformations and in normal control participants.** *AJNR Am J Neuroradiol* 2003;24:169–76
- Iskandar BJ, Quigley M, Houghton VM. **Foramen magnum cerebrospinal fluid flow characteristics in children with Chiari I malformation before and after craniocervical decompression.** *J Neurosurg* 2004;101(2 suppl):169–78
- Quigley MF, Iskandar B, Quigley ME, et al. **Cerebrospinal fluid flow in foramen magnum: temporal and spatial patterns at MR imaging in volunteers and in patients with Chiari I malformation.** *Radiology* 2004;232:229–36
- Bateman GA. **Vascular compliance in normal pressure hydrocephalus.** *AJNR Am J Neuroradiol* 2000;21:1574–85
- Bateman GA, Loisele AM. **Can MR measurement of intracranial hydrodynamics and compliance differentiate which patient with idiopathic normal pressure hydrocephalus will improve following shunt insertion?** *Acta Neurochir (Wien)* 2007;149:455–62, discussion 462
- Balédent O, Henry-Feugeas MC, Idy-Peretti I. **Cerebrospinal fluid dynamics and relation with blood flow: a magnetic resonance study with semiautomated cerebrospinal fluid segmentation.** *Invest Radiol* 2001;36:368–77
- Henry-Feugeas MC, Idy-Peretti I, Baledent O, et al. **Cerebrospinal fluid flow waveforms: MR analysis in chronic adult hydrocephalus.** *Invest Radiol* 2001;36:146–54
- Kahlon B, Annertz M, Ståhlberg F, et al. **Is aqueductal stroke volume, measured with cine phase-contrast magnetic resonance imaging scans useful in predicting outcome of shunt surgery in suspected normal pressure hydrocephalus?** *Neurosurgery* 2007;60:124–29, discussion 129–30
- Scollato A, Tenenbaum R, Bahl G, et al. **Changes in aqueductal CSF stroke volume and progression of symptoms in patients with unshunted idiopathic normal pressure hydrocephalus.** *AJNR Am J Neuroradiol* 2008;29:192–97
- Egnor M, Zheng L, Rosiello A, et al. **A model of pulsations in communicating hydrocephalus.** *Pediatr Neurosurg* 2002;36:281–303
- Branco G, Goulão A, Ferro JM. **MRI in aqueduct compression and obstructive hydrocephalus due to an ectatic basilar artery.** *Neuroradiology* 1993;35:447–48
- Bradley WG. **Cerebrospinal fluid dynamics and shunt responsiveness in patients with normal-pressure hydrocephalus.** *Mayo Clin Proc* 2002;77:507–08
- Yamada S, Miyazaki M, Kanazawa H, et al. **Visualization of cerebrospinal fluid movement with spin labeling at MR imaging: preliminary results in normal and pathophysiologic conditions.** *Radiology* 2008;249:644–52
- Miyazaki M, Lee VS. **Nonenhanced MR angiography.** *Radiology* 2008;248:20–43
- Chen X, Xia C, Sun J, et al. **Nonenhanced renal artery MR angiography with time spatial labeling inversion pulse technology and its clinical values[in Chinese].** *Sichuan Da Xue Xue Bao Yi Xue Ban* 2010;41:881–84
- Hori M, Aoki S, Oishi H, et al. **Utility of time-resolved three-dimen-**



- sional magnetic resonance digital subtraction angiography without contrast material for assessment of intracranial dural arterio-venous fistula. *Acta Radiol* 2011;52:808–12
41. Ishimori Y, Monma M, Kawamura H, et al. Time spatial labeling inversion pulse cerebral MR angiography without subtraction by use of dual inversion recovery background suppression. *Radiol Phys Technol* 2011;4:78–83
  42. Kogure T, Kogure K, Iizuka M, et al. Effective use of flow-spoiled FBI and time-SLIP methods in the diagnostic study of an aberrant vessel of the head and neck: “left jugular venous steal by the right jugular vein.” *J Magn Reson Imaging* 2010;32:429–33
  43. Satogami N, Okada T, Koyama T, et al. Visualization of external carotid artery and its branches: non-contrast-enhanced MR angiography using balanced steady-state free-precession sequence and a time-spatial labeling inversion pulse. *J Magn Reson Imaging* 2009;30:678–83
  44. Sugita R, Furuta A, Horaguchi J, et al. Visualization of pancreatic juice movement using unenhanced MR imaging with spin labeling: preliminary results in normal and pathophysiologic conditions. *J Magn Reson Imaging* 2012;35:1119–24
  45. Yamada S, Goto T. Understanding of cerebrospinal fluid hydrodynamics in idiopathic hydrocephalus (A) visualization of CSF bulk flow with MRI time-spatial labeling pulse method (time-SLIP) [in Japanese]. *Rinsho Shinkeigaku* 2010;50:966–70
  46. Yamada S, Shibata M, Scadeng M, et al. MRI tracer study of the cerebrospinal fluid drainage pathway in normal and hydrocephalic guinea pig brain. *Tokai J Exp Clin Med* 2005;30:21–29
  47. Yamada S, Goto T, McComb JG. Use of a spin-labeled cerebrospinal fluid magnetic resonance imaging technique to demonstrate successful endoscopic fenestration of an enlarging symptomatic cavum septi pellucidi. *World Neurosurg* 2013;80:436.e15–18
  48. Shaw CM, Alvord EC Jr. Cava septi pellucid et vergae: their normal and pathological states. *Brain* 1969;92:213–23
  49. Yamada S, Miyazaki M, Yamashita Y, et al. Influence of respiration on cerebrospinal fluid movement using magnetic resonance spin labeling. *Fluids Barriers CNS* 2013;10:36